Proc. Natl. Acad. Sci. USA
Vol. 87, pp. 8560–8564, November 1990
Genetics

Initiation of rolling-circle replication in pT181 plasmid: Initiator protein enhances cruciform extrusion at the origin

(DNA secondary structure/bromoacetaldehyde/S1 nuclease/origin utilization)

PHILIPPE NOIROT*, JILL BARGONETTI, AND RICHARD P. NOVICK

Public Health Research Institute, 455 First Avenue, New York, NY 10016

Communicated by Arthur Kornberg, May 15, 1990

ABSTRACT **Plasmid pT181 DNA secondary structures have been analyzed *in vitro* by nuclease S1 digestion and *in vivo* by bromoacetaldehyde treatment. A cruciform structure occurring at the pT181 replication origin *in vitro* is greatly enhanced by the binding of the plasmid-encoded initiator protein RepC. *In vivo* a DNA secondary structure also existed in the replication origin. Its frequency of formation was correlated with efficiency of RepC utilization. These data suggest that cruciform extrusion at the origin is involved in initiation of pT181 rolling-circle replication. A neighboring DNA structure influences the conformation of the origin *in vivo*.**

Small staphylococcal plasmids replicate by means of an asymmetric rolling-circle mechanism, initiated by a plasmid-encoded protein that introduces a site-specific nick (for review, see ref. 1). The pT181 initiator protein binds to and nicks both single-stranded and double-stranded DNA containing its recognition site (2). However, replication is initiated only when the DNA is supercoiled (3).

Analysis of plasmid pT181 DNA secondary structure has revealed a cruciform structure at the replication origin; formation of this cruciform was greatly enhanced by binding of the plasmid-coded initiator protein RepC. Bromoacetaldehyde treatment of whole cells has revealed a similar structure *in vivo*; frequency of formation of this structure was influenced by other secondary structures and correlated with efficiency of RepC use. Initiation of replication may proceed by means of this origin cruciform. Such a hypothesis suggests that a locally denatured region of the origin is required for the entry of initiation factors in rolling-circle replication, as for θ replication (4, 5). In pT181, the leading-strand origin is highly G+C rich, making it an unlikely site for local superhelix-driven denaturation. However, as for certain other rolling-circle origins, a strong potential hairpin is present and is necessary for origin function; origin activity is decreased by mutations that destabilize the hairpin and is eliminated by deletion of the symmetry element. Accordingly, we hypothesized that unwinding of this G+C-rich region could be initiated by superhelix-driven formation of this cruciform structure.

We show here that the predicted cruciform in the pT181 leading-strand origin forms *in vitro* and that its formation is enhanced by binding of the initiator protein RepC. A secondary structure that probably corresponds to this cruciform also forms *in vivo*. Elimination of competing secondary structures elsewhere in the plasmid increased both the frequency of cruciform extrusion at the origin and the efficiency of origin use *in vivo*. These results suggest that initiator-enhanced cruciform extrusion provides the single-stranded region necessary for assembly of the replication complex.

The publication costs of this article were defrayed in part by page charge payment. This article must therefore be hereby marked "*advertisement*" in accordance with 18 U.S.C. §1734 solely to indicate this fact.

MATERIALS AND METHODS

Bacterial Strains and Plasmids. The strains used were derivatives of *Staphylococcus aureus* NTCC8325 (8). Plasmids used were pT181 (9) and its copy mutants pT181 *cop-608* and *cop-623* (10).

General Methods. Media for *S. aureus* were used as described (10). Tetracycline was used at 5 μg/ml. Supercoiled plasmid DNA was isolated as described (11).

Manipulation of DNA. Enzymes were purchased from Bethesda Research Laboratories and Boehringer Mannheim. Radiolabeled probes were prepared by nick-translation (12). DNA was sequenced by the dideoxynucleotide chain-termination method (13).

Mapping of S1 Nuclease-Sensitive Sites. Supercoiled plasmid DNA was preincubated in 10 mM Tris·HCl, pH 7.0/1 mM EDTA for 30 min at 37°C. The buffer was adjusted to 33 mM sodium acetate, pH 4.6/100 mM NaCl/1 mM $ZnCl_2$, and S1 nuclease was added at 0.5–1 unit per μg of DNA. Under these conditions S1 nuclease produces either nicked or linear molecules depending on incubation time. S1 nuclease-sensitive sites were mapped by determining double-stranded cleavage sites and then sequencing nicks induced by S1 nuclease at corresponding locations. Linear molecules were generated by incubation for 45 min at 37°C. The reaction was stopped by adding EDTA, and the DNA was phenol-extracted, ethanol-precipitated, and digested with a restriction enzyme that cleaved the plasmid once. The resulting fragments were analyzed by agarose gel electrophoresis. Singly nicked molecules were generated by incubation for 10 min at 37°C. The DNA was treated as above and then digested with *Taq* I or *Rsa* I. A restriction fragment containing a previously localized S1 nuclease site was isolated by PAGE, treated with alkaline phosphatase, and 5′ end-labeled with polynucleotide kinase and [γ-^{32}P]ATP. The label at one end was removed by digestion with a second restriction enzyme. The subfragment of interest was isolated, denatured, and subjected to electrophoresis on 8% polyacrylamide-urea gel.

Mapping of Bromoacetaldehyde-Sensitive Sites *in Vivo*. Bromoacetaldehyde was prepared as described (14). Bromoacetaldehyde reacts only with the amino groups of unpaired adenine and cytosine residues; the bromoacetaldehyde-modified bases cannot reestablish Watson–Crick pairing and so retain S1 nuclease sensitivity (14). Cultures in mid-exponential phase at 37°C were treated with 100 mM bromoacetaldehyde for 30 min at 37°C. Four-microgram samples of supercoiled plasmid DNA prepared from treated and untreated cells were linearized with a singly cutting restriction enzyme, treated with 10 units of S1 nuclease per μg of DNA for 10 min at 22°C, separated by agarose gel electrophoresis, and blot-hybridized (12) with a pT181 probe.

Abbreviations: nt, nucleotide(s); IR-II, inverted repeat II.

*Present address: Laboratoire de Genetique Microbienne, Institut National de la Recherche Agronomique, Domaine de Vilvert, 78350 Jouy en Josas, France.

Detection of DNA Secondary Structures upon RepC Binding *in Vitro*. Three and a half micrograms of supercoiled pT181 plasmid DNA in 50 mM Tris·HCl, pH 7.5/1 mM dithiothreitol/1 mM EDTA was incubated for 30 min at 37°C with various amounts of purified RepC (15) and then with bromoacetaldehyde (50 mM final concentration) for 60 min. After phenol extraction and ethanol precipitation, the DNA was linearized with a singly cutting restriction enzyme, digested with S1 nuclease (1 unit per μg of DNA), and analyzed by agarose gel electrophoresis.

Measurement of RepC Synthesis *in Vivo*. The structural gene for β-lactamase (*blaZ*) from *S. aureus* plasmid pI258 was translationally coupled to the 3′ end of *repC* in the intact pT181 plasmid using the overlapping stop–start sequence ATGA. Both proteins are synthesized in native form, and the plasmid copy number is unaffected (J.B. and R.P.N., unpublished work). β-Lactamase activities (16) were used to calculate the relative rates of RepC production as described (17).

RESULTS

Because the secondary structure of pT181 DNA was not known, we mapped sites of sensitivity to single-strand probes *in vitro*, then evaluated the effects of deletion and initiator protein binding, and finally examined the structure of the plasmid *in vivo*.

Mapping of S1 Nuclease-Sensitive Sites. Treatment of supercoiled DNA by S1 nuclease and a singly cutting restriction enzyme produced many pairs of fragments arising from molecules linearized by S1 nuclease at different sites (Fig. 1). We considered only the most intense fragments to represent S1 nuclease sites of interest; the background fragments probably arose from the cutting of randomly denatured regions. As only a small fraction of the molecules will contain any particular secondary structure at digestion, smaller bands are faint and, therefore, not well reproduced in the photographs. Simultaneous analysis of the patterns produced by two singly cutting restriction enzymes allowed localization of S1 nuclease sites to within 100–200 nucleotides (nt). In wild-type pT181 DNA (Fig. 1 *Left*) and in pT181 *cop-608* DNA the major S1-sensitive site, α, is located in the copy control region between nt 200 and 300 (Fig. 2). The weaker S1 nuclease site, β, is located between nt 30 and 110 in the region of replication origin. In pT181 *cop-608* DNA (Fig. 1 *Right*) (deletion of nt 184–363), the α site was missing, and the S1 sensitivity of several weaker sites was enhanced. The strongest of these sites corresponds to site β, which gives rise to fragments of 0.8 kilobase (kb) in the S1–*Cla* I codigest and 1.6 kb in the S1–*Eco*RV codigest that are also present in wild-type pT181. Two additional minor sites, γ and δ, occurred at 2000 ± 100 bp and 3600 ± 100 bp, respectively, near or within the *pre* and *tet* promoters, respectively (18, 19). γ is near or within the *pre* promoter (18); δ is near or within the *tet* promoter (19) (see Fig. 2).

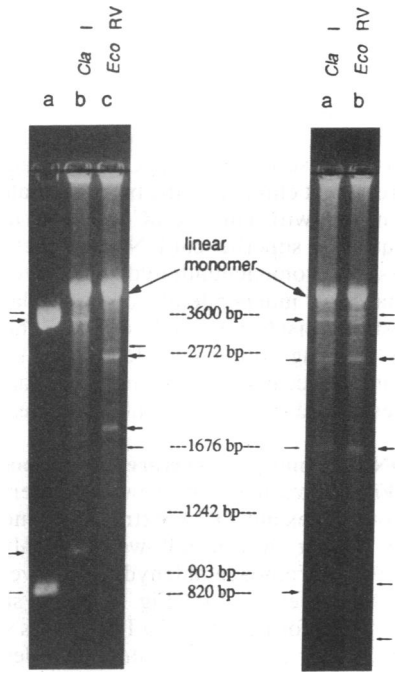

FIG. 1. Mapping of S1 nuclease double-stranded cutting sites. Bands smaller than the linear monomer correspond to S1 nuclease cutting sites. Major sites are shown by thick arrows, and minor sites are shown by thin arrows. (*Left*) Size marker pT181 wild type codigested with *Cla* I and *Hpa* II (lane a). pT181 wild type was digested with *Cla* I (lane b) and *Eco*RV (lane c). (*Right*) pT181 *cop-608* was digested with *Cla* I (lane a) and *Eco*RV (lane b). An S1 nuclease cut in the replication origin will produce an 820-base pair (bp) fragment after *Cla* I digestion and a 1620-bp fragment after *Eco*RV digestion.

The major site in wild-type pT181 DNA was resolved at the nucleotide level into two nearby sites, α at nt 229–233 and α′ at nt 371–375 (Figs. 3 and 4). Site α is located in the −10 sequence of the countertranscript promoter (20). Site α′ is located in the major *repC* promoter that overlaps the transcription terminator for the longer countertranscript, RNA II (see Fig. 4). The two strands were nicked symmetrically at the center of palindromic sequences in both sites and with roughly the same frequency. α′, unlike α, was not detected as a double-stranded S1 nuclease cutting site, implying that S1 nuclease does not cleave from across a nick. The major site in *cop-608* DNA was also resolved at the nucleotide level into two closely linked sites, corresponding to β and α′ in the wild type (see Fig. 3). In this case, only the bottom strand was analyzed. The β site, at nt 68–74, was located at the center of IR-II, which includes the RepC nicking site (between nt 70 and 71) (see Fig. 4). The α′ site (nt 375–378) was displaced compared with the corresponding α′ site (nt 371–375) in wild-type DNA and did not correspond to nucleotides predicted to be single stranded. Indeed, the *cop-608* deletion reduces the size and complementarity of the inverted repeat at this site, greatly weakening the potential hairpin.

Initiator Protein Binding Unwinds the Replication Origin. The existence of the IR-II cruciform (the β site) in pT181 DNA suggested that this structure might be the primary substrate for the initiation of leading-strand replication. Consistent with this possibility were experiments showing that

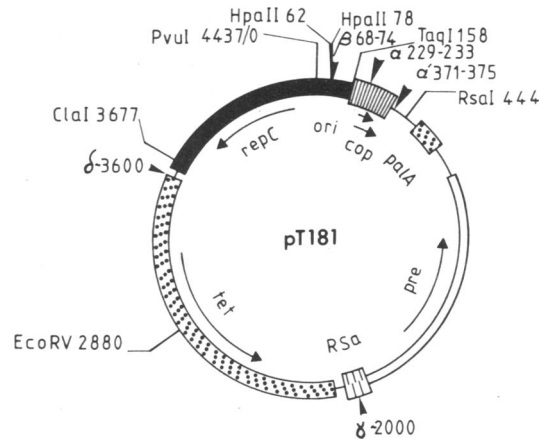

FIG. 2. Location of S1 nuclease sites on pT181 genetic map. Thin arrows inside circle indicate direction of transcription of the three major open reading frames and of the countertranscripts (cop) (9, 20). Locations of the S1 nuclease sites are shown by the arrowheads; their sizes indicate relative S1 nuclease sensitivity.

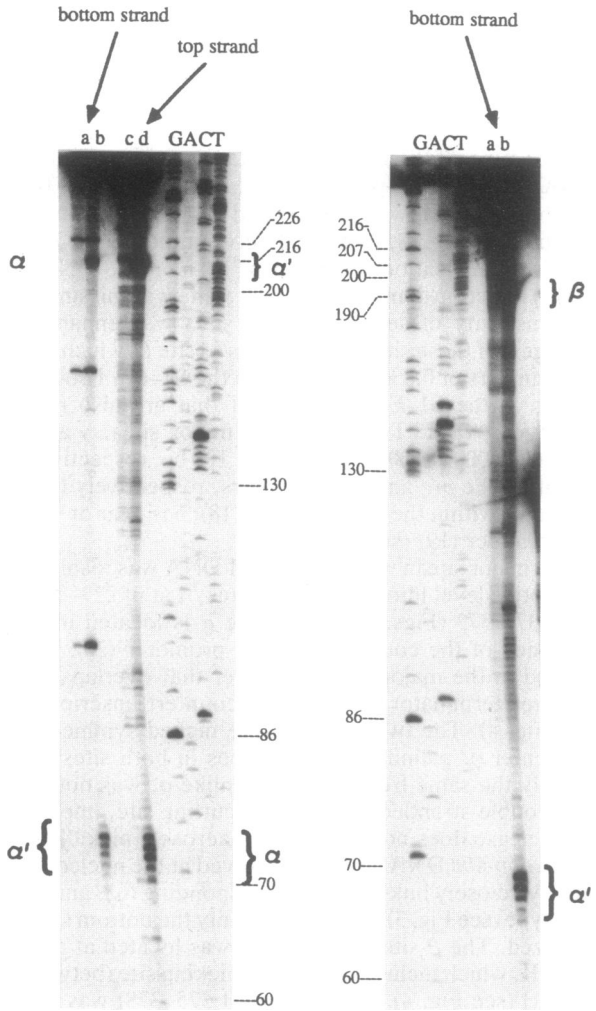

FIG. 3. Localization of the S1 nuclease-sensitive sites. S1 nicking sites are characterized by clusters of bands with 1-nt spacing, marked by the brackets. (*Left*) Localization of the α site on pT181 wild-type DNA. Fragment *Taq* I (position 158)–*Rsa* I (position 444), labeled at the *Rsa* I site, was used for the bottom strand, and for the top strand this fragment was labeled at the *Taq* I site. Lanes: a and c, plasmid DNA not treated with S1 nuclease; b and d, plasmid DNA treated with S1 nuclease; G, A, T, and C, sequencing ladders prepared by the dideoxynucleotide chain-termination method on a pT181 wild-type template with primer 5′ (position 455) → 3′ (position 438). Lengths of relevant bands are indicated in bp. (*Right*) Localization of the β site in *cop-608* DNA. The fragment *Pvu* I (position 1)–*Rsa* I (position 444), labeled at the *Rsa* I site, was used for the bottom strand only. Lanes: G, A, T, and C, sequencing ladders as described; a, plasmid DNA not treated with S1 nuclease; b, plasmid DNA treated with S1 nuclease. Bands corresponding to the β site, well visualized in the original autoradiogram, are obscured by the highly labeled intact *Pvu* I–*Rsa* I fragment.

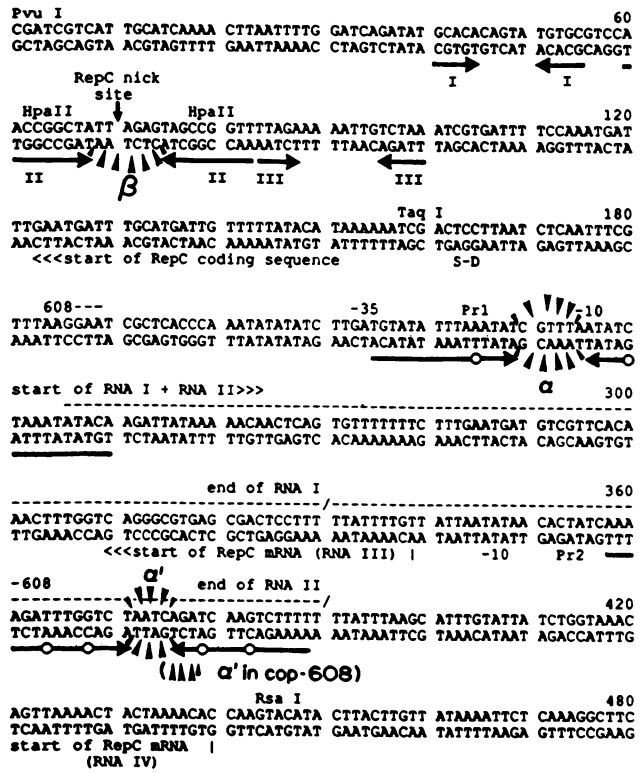

FIG. 4. Summary of S1 nuclease mapping data. Nucleotide sequence of the pT181 replication origin and copy control region (nt 1–480) is represented with features such as the extent of the *cop-608* deletion, transcriptional initiation points, locations of the RepC nicking site, and useful restriction sites. Short clustered arrowheads represent the S1 nicking sites (α, α′, and β) on the indicated strands, corresponding to the clusters of bands seen in Fig. 3. Inverted repeats are indicated by horizontal arrows and, within the replication origin, IR-I, -II, -III are shown.

RepC enhanced cruciform extrusion at the leading-strand origin, as shown in Fig. 5. Here, the frequency of appearance of the β-site cruciform was monitored as a function of RepC concentration. Mg^{2+} was omitted from the reaction mixture, which allowed normal binding but prevented nicking (21). To compare the results of the *in vivo* analysis (below), we used bromoacetaldehyde. After treatment, RepC and bromoacetaldehyde were removed, and pT181 *cop-608* DNA was linearized with *Eco*RV (Fig. 5, lanes c–p) and digested with S1 nuclease. As shown in lanes c–n, binding of RepC to the DNA before bromoacetaldehyde treatment increased sensitivity of the origin to bromoacetaldehyde. The concentration effect was seen only at a molar ratio of RepC to DNA <2. Omission of bromoacetaldehyde eliminated the effect (lane p), thus showing that S1 nuclease cleaves only at bromoacetaldehyde-modified sites. Relaxation of the DNA by calf thymus topoisomerase I before RepC binding and bromoacetaldehyde treatment eliminated the bromoacetaldehyde sensitivity (data not shown). Thus, RepC-mediated unwinding of the origin requires a superhelical DNA molecule. The other bands represent bromoacetaldehyde-sensitive secondary structures that form independently of RepC (lane d). Note that these results considerably underestimate the proportion of molecules showing bromoacetaldehyde sensitivity at the replication origin because coexisting bromoacetaldehyde-modified sites would cause different S1 nuclease cleavage patterns.

***In Vivo* DNA Secondary Structures Correspond to Those Existing *in Vitro*.** Treatment of growing bacteria with bromoacetaldehyde, plasmid DNA extraction, and restriction with a singly cutting enzyme followed by analysis with S1 nuclease revealed bromoacetaldehyde-sensitive sites corresponding to those seen *in vitro* (Fig. 6). Analysis with *Cla* I and *Eco*RV was performed; the *Cla* I pattern is shown. With pT181 *cop-623*, only the α and γ sites were detected (*Left*, lane f), whereas with pT181 *cop-608*, β and γ were detected (*Right*, lane e). The δ site was not detected in these experiments, probably because of the lower sensitivity of the method *in vivo*. The hierarchy of secondary structures *in vivo* was similar to that observed *in vitro*, except that the γ structure was not suppressed by α.

Secondary Structure of Plasmid DNA Is Correlated with Efficiency of RepC Use *in Vivo*. That RepC enhancement of cruciform extrusion at the replication origin occurs *in vivo* was supported by demonstrating that pT181 *cop-608*, which shows

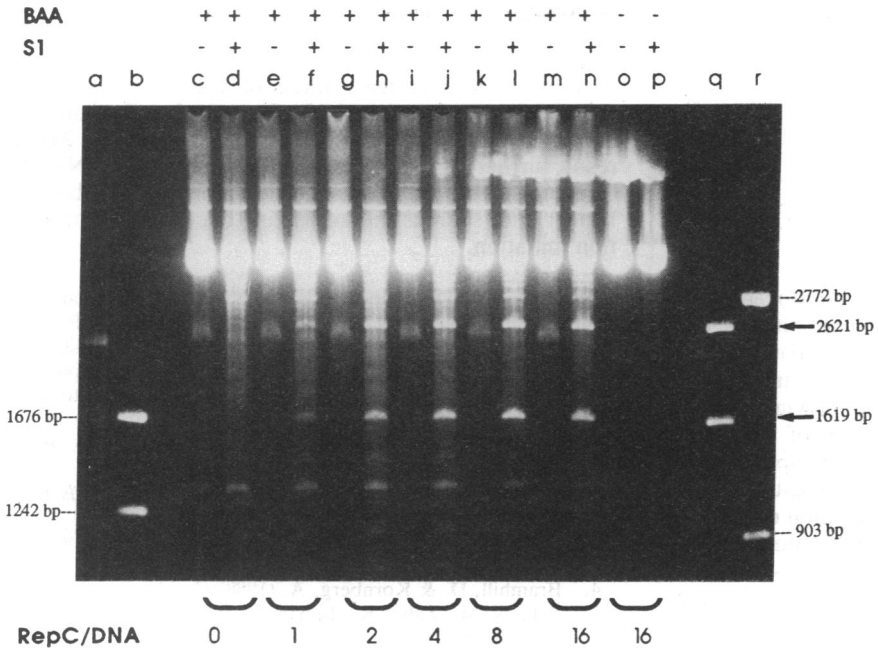

FIG. 5. Enhancement of bromoacetaldehyde (BAA) sensitivity at the replication origin upon RepC binding *in vitro*. Lanes: c–p, bromoacetaldehyde and S1 nuclease treatments are indicated at top. Markers were supercoiled monomer (lane a) and linear-sized (lanes b, q, and r). Arrows indicate cut in replication origin. See text for details.

a DNA secondary structure in the replication origin *in vivo*, uses RepC more efficiently than pT181 *cop-623*, which does not. Estimation of efficiency of initiation is given by the relative rate of RepC synthesis and, presumably, utilization per plasmid copy per generation. Table 1 shows that in *S. aureus* containing pT181 *cop-608*, <0.5 as much RepC is synthesized per plasmid copy than in the same strain containing pT181 *cop-623*. The results suggest that pT181 *cop-608* uses RepC more than twice as efficiently as pT181 *cop-623*. Therefore, the bromoacetaldehyde-sensitive structure at the replication origin in pT181 *cop-608*, which probably corresponds to the IR-II cruciform, may be involved in initiation.

DISCUSSION

Role of the IR-II Cruciform in the Leading-Strand Initiation. In this work, we demonstrated a conformational change in

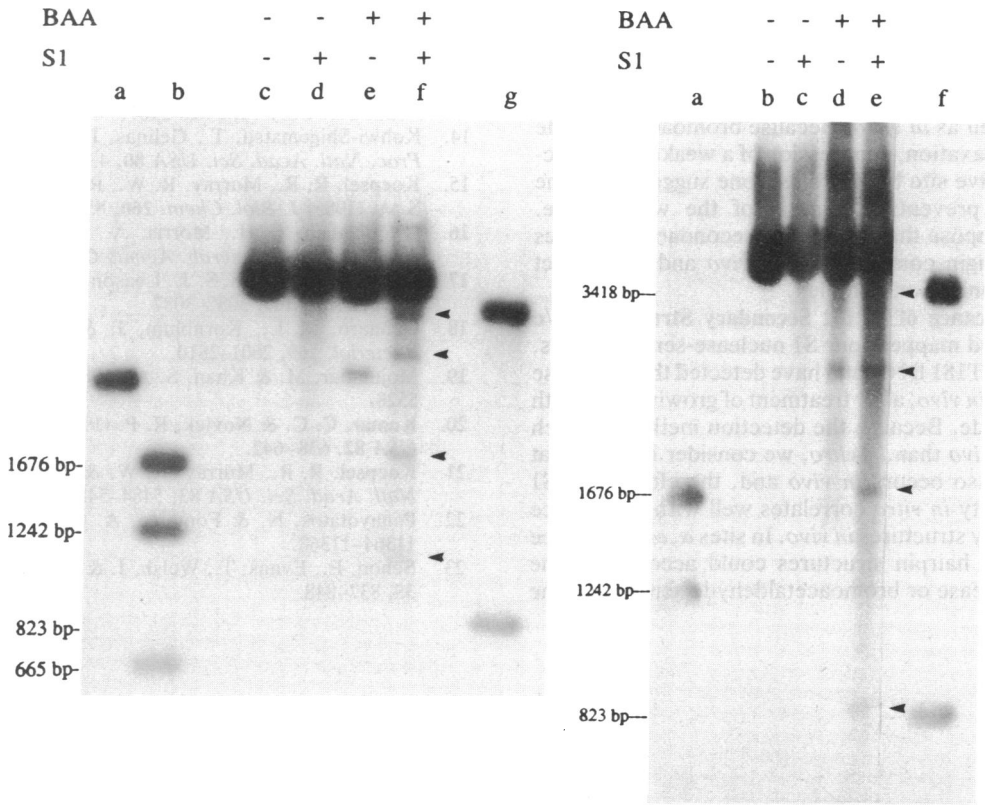

FIG. 6. *In vivo* mapping of the bromoacetaldehyde-sensitive sites. Treatments are indicated at top. Arrowheads indicate fragments produced by treatment with both bromoacetaldehyde and S1 nuclease. (*Left*) pT181 *cop-623* DNA. Lanes: a, supercoiled monomers; b, *Rsa* I digest; c–f, *Cla* I digest; g, *Cla* I plus *Hpa* II codigest. (*Right*) pT181 *cop-608* DNA. Lanes: a, pT181 wild-type *Rsa* I digest; b–e, *Cla* I digest; f, *Cla* I plus *Hpa* II codigest. Note that bands resulting from codigestions involving *Hpa* II correspond to bromoacetaldehyde S1 nuclease cutting at the replication origin.

Table 1. RepC utilization vs. unwinding at the origin *in vivo*

	pT181	pT181 *cop-623*	pT181 *cop-608*
Copy number (21)	20–25	400–500	800–1000
Unwinding *in vivo*		–	+
RepC synthesis rate*	16	290	260
RepC/plasmid copy†	0.64–0.80	0.58–0.73	0.26–0.32

*Milliunits of β-lactamase activity per mg of dry weight.
†RepC synthesis rate per plasmid copy number.

the leading-strand origin of pT181 upon initiator protein binding. Location of the S1 nuclease cleavage sites at the center of the IR-II palindrome indicated formation of a cruciform structure, enhanced by RepC binding and dependent on superhelicity. We suggest that this unwinding corresponds to RepC induction or stabilization of the IR-II cruciform. Extrusion of the IR-II cruciform upon RepC binding may be required for initiation of replication. This structure could provide the single-stranded region necessary for entry of host initiation proteins into the DNA duplex. The hypothesis implies that RepC nicking of molecules destined to replicate would occur in the single-stranded loop of the cruciform. The ability of RepC to nick specifically a single-stranded oligonucleotide containing the IR-II sequence (2) is consistent with this model. *In vivo*, a secondary structure in the replication origin was detected in pT181 *cop-608*, in which a competing DNA structure located in the copy control region had been deleted but not in pT181 *cop-623*, which contains this competing structure. This result correlates with a lower rate of RepC production per copy for the former plasmid—which we interpret to mean that RepC is more efficiently used. That is, the greater the frequency of IR-II extrusion, the more efficient the use of the initiator for replication. We note that a native cruciform of unknown biological significance has been detected *in vivo* in the plasmid ColE1 gene encoding colicin immunity (22).

The hierarchical relationship between sites α and β was seen *in vivo* as well as *in vitro*. Because bromoacetaldehyde does not cause relaxation, suppression of a weaker bromoacetaldehyde-sensitive site by a stronger one suggests that the strong structure prevents formation of the weaker one. Therefore, we propose that competing secondary structures may influence origin conformation *in vivo* and thus affect formation of the initiation complex.

Possible Significance of pT181 Secondary Structures. We have identified and mapped four S1 nuclease-sensitive sites, α, β, γ, and δ, in pT181 DNA and have detected three of these sites, α, β, and γ, *in vivo*, after treatment of growing cells with bromoacetaldehyde. Because the detection method is much less sensitive *in vivo* than *in vitro*, we consider it likely that the δ structure also occurs *in vivo* and, therefore, that S1 nuclease sensitivity *in vitro* correlates well with occurrence of DNA secondary structures *in vivo*. In sites α, α′, and β (see Fig. 4), potential hairpin structures could account for the observed S1 nuclease or bromoacetaldehyde sensitivity; the positions that are attacked would be single-stranded in these hairpins.

In summary, DNA secondary structures were detected *in vivo* in or near at least three of the four major pT181 promoters, consistent with the frequent localization of secondary structures to promoter regions *in vitro* (6, 23). This result further supports the hypothesis that the DNA structures detected with bromoacetaldehyde *in vivo* play a biological role, such as the unwinding necessary for transcription initiation.

We thank Karl Drlica and Maria L. Gennaro for advice and critical reading of this manuscript, S. J. Projan, M. F. Gros, and P. Z. Wang for stimulating discussions, S. Moghazeh for technical assistance, and D. Everett for administrative support. This work was supported by a grant from the National Institutes of Health (GM 14372) to R.P.N.

1. Gruss, A. D. & Ehrlich, S. D. (1989) *Microbiol. Rev.* **53**, 231–241.
2. Koepsel, R. R. & Khan, S. A. (1987) *Nucleic Acids Res.* **15**, 4085–4097.
3. Khan, S. A., Carleton, S. M. & Novick, R. P. (1981) *Proc. Natl. Acad. Sci. USA* **78**, 4902–4906.
4. Bramhill, D. & Kornberg, A. (1988) *Cell* **52**, 743–755.
5. Schnos, M., Zahn, K., Inman, R. B. & Blattner, F. R. (1988) *Cell* **52**, 385–395.
6. Drew, H. R., Weks, J. R. & Travers, A. A. (1985) *EMBO J.* **4**, 1025–1032.
7. Gennaro, M. L., Iordanescu, S., Novick, R. P., Murray, R. W., Steck, T. R. & Khan, S. A. (1989) *J. Mol. Biol.* **205**, 355–362.
8. Novick, R. P. (1967) *Virology* **33**, 155–166.
9. Khan, S. A. & Novick, R. P. (1983) *Plasmid* **10**, 151–159.
10. Carleton, S., Projan, S. J., Highlander, S. K., Moghazeh, S. & Novick, R. P. (1984) *EMBO J.* **3**, 2407–2414.
11. Novick, R. P., Murphy, E., Gryczan, T. J., Baron, E. & Edelman, I. (1979) *Plasmid* **2**, 109–129.
12. Maniatis, T., Fritsch, E. F. & Sambrook, J. (1982) *Molecular Cloning: A Laboratory Manual* (Cold Spring Harbor Lab., Cold Spring Harbor, NY).
13. Sanger, F., Nicklen, S. & Coulson, A. R. (1977) *Proc. Natl. Acad. Sci. USA* **74**, 5463–5467.
14. Kohwi-Shigematsu, T., Gelinas, R. & Weintraub, H. (1983) *Proc. Natl. Acad. Sci. USA* **80**, 4389–4393.
15. Koepsel, R. R., Murray, R. W., Rosenblum, W. D. & Khan, S. A. (1985) *J. Biol. Chem.* **260**, 8571–8577.
16. O'Callaghan, C. H., Morris, A., Kirby, S. M. & Shingler, A. H. (1972) *Antimicrob. Agents Chemother.* **1**, 283–288.
17. Wang, P. Z., Projan, S. J., Leason, K. & Novick, R. P. (1987) *J. Bacteriol.* **169**, 3082–3087.
18. Gennaro, M. L., Kornblum, J. & Novick, R. P. (1987) *J. Bacteriol.* **169**, 2601–2610.
19. Mojumdar, M. & Khan, S. A. (1988) *J. Bacteriol.* **170**, 5522–5528.
20. Kumar, C. C. & Novick, R. P. (1985) *Proc. Natl. Acad. Sci. USA* **82**, 638–642.
21. Koepsel, R. R., Murray, R. W. & Khan, S. A. (1986) *Proc. Natl. Acad. Sci. USA* **83**, 5484–5488.
22. Panayotatos, N. & Fontaine, A. (1987) *J. Biol. Chem.* **262**, 11364–11368.
23. Schon, E., Evans, T., Welsh, J. & Efstratiadis, A. (1983) *Cell* **35**, 837–848.